Proceeding of the IEEE
International Conference on Robotics and Biomimetics
Dali, China, December 2019

Kinematic Optimization of Tendon-sheath Actuated Hand

Meng Yin[1,2,3], Wei Han[1,2,4], Zhigang Xu[1,2], Haoting Wu[1,2,4], Zhiliang Zhao[1,2,4]

1. Shenyang Institute of Automation, Chinese Academy of Sciences, Shenyang 110016, China
2. Institutes for Robotics and Intelligent Manufacturing, Chinese Academy of Sciences, Shenyang 110169, China
3. University of Chinese Academy of Sciences, Beijing 100049, China
4. School of Mechanical Engineering and Automation, Northeastern University, Shenyang110169, China
Corresponding author: Meng. Yin (yinmenglz@163.com).

***Abstract* - With the continuous development of robot applications, humanoid dexterous hands has become an important research direction. In this paper, a five-finger humanoid dexterous hand is designed. The tendon-sheath transmission is applied, which avoids the coupling between the joints. The dexterous hand is comprised of 19 degrees of freedom. Built on the concept of bionics, the dexterous hand is designed and the inverse kinematics of the dexterous hand is analyzed. And then, the relevant parameters of the hand are optimized with the targets of dexterity and the maximizing grabbing space. The optimized parameters were used in the manufacture, and the rationality of design was verified by experiments of flexibility and grasping ability.**

***Index Terms* - Dexterous hand • Decoupling degrees of freedom • Minimum singular value • Relative shape closure.**

I. INTRODUCTION

Dexterous hands can be divided into industrial dexterous hands and humanoid dexterous hands[1]. Humanoid multi-finger dexterous hand can be used not only as a general-purpose operating device in various fields, but also as a prosthetic for disabled people, and has significant social application value[2].

The representative of the built-in motor drive is DLR-HIT and II [3]. The operation of the DLR-II is relatively simple, and the degree of integration and modularity is high. However, compared with additional driving methods, it increases the harmonic gear reducer in order to achieve the high torque of the joint, being a little bit more cumbersome. Similar dexterous hands are including the Spanish MA-1[4], the American Barret hand [5], and the Japanese Gifu Hand [6].

The artificial muscle-driven methods are represented by Shadow Hand [7]. Its driving source comes from a pneumatic device called "air muscle" made by the company of Shadow. Report to the motor-driven dexterous hand, its power part is relatively straightforward, the finger movement is more human-like, and there is no other posture that is not in line with the human hand structure. However, they have the problems of unstable pneumatic muscles, high temperature and high cost. Similar dexterous hands are including the Japanese Tokyo hand [8] and Ultralight hand [9].

The representative of the tendon drive mode is the Robonaut hand [10]. Compared with the DLR-II, which uses a motor as a dual drive, the tendon drive has the characteristics of small size, large torque and long force transmission distance. At the same time, because the driver is far away from the palm of the hand, the weight of the palm is very light, and the noise of driving the joint movement of the finger is also much smaller than that of the DLR-II. Similar dexterous hands are including Italian UBH3 hand [11] and the French LMS hand [12].

There are numerous unique advantages of the tendon drive compared to other drive methods. For example, the driver can be separated the palm, so that the structure becomes compact. This paper designs a five-finger humanoid dexterous hand based on the bionics principle. Improved transmission of the tendon drive avoids coupling between the joints. Kinematics of dexterous hand is analyzed, and mechanism parameters are designed with the Jacques condition index and the maximizing the grabbing space as the optimization goal. The optimized parameters were adopted in the manufacture of physical objects. The rationality of design schemes and parameters was verified by experiments of flexibility and grasping ability.

II. THE PRINCIPLE AND STRUCTURE OF DEXTEROUS HAND

The base joint of the dexterous hand uses a double lasso transmission because of its ability to move in both directions. The metal hose wrapping the wire rope is fixed on the joint, and the wire rope a is driven by the driving wheel, passes through the pre-tightening mechanism, enters the metal hose, and then connects with the driven wheel. The wire rope b is driven by the driven wheel, first enters the metal hose, and then is pre-tightened with the driving wheel by the pre-tightening mechanism.

Except for the base joint, the rest of the fingers are unidirectional load movement, so a single lasso model can be used. The structure differs from the double lasso in that the torsion spring replaces the wire rope b, as shown in Fig. 1.

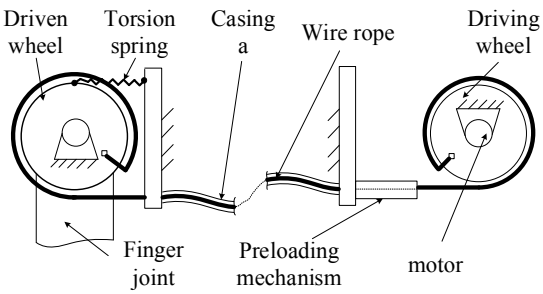

Fig. 1 Single Tendon-sheath Transmission System

978-1-7281-6321-5/19//$31.00 ©2019 IEEE

Due to the complexity of the human hand, the current technology is difficult to perfectly reproduce the human hand movement. Moreover, some of the more complicated functions of human hands are lower in daily life and are not commonly used. Therefore, domestic and foreign scholars have extracted several kinds of grasping postures with high usage rate by studying the methods of grasping human hands in daily life. This allows the robot to complete more grabbing tasks with limited gripping posture. The more freedom, the better the flexibility, the design of the dexterous hand has a total of 19 degrees of freedom, as shown in Fig 2. The index finger, the middle finger, the ring finger and the little finger respectively have 4 degrees of freedom, wherein the lower degree of freedom is the swinging degree of freedom, and the upper three degrees of freedom are the degree of freedom of bending. Due to the appearance limitation, the thumb design has 3 degrees of freedom, and the upper two degrees of freedom are bending degrees of freedom. The components are made of 3D printed nylon material, which is driven by a stern and a steering gear and wire rope. The dexterous hand's grasping ability is related to the design of the degree of freedom, and to the position of the swinging degree of freedom of the thumb and the size of each finger.

The dexterous hand experiment system is mainly composed of power source, control system, dexterous hand and transmission system.

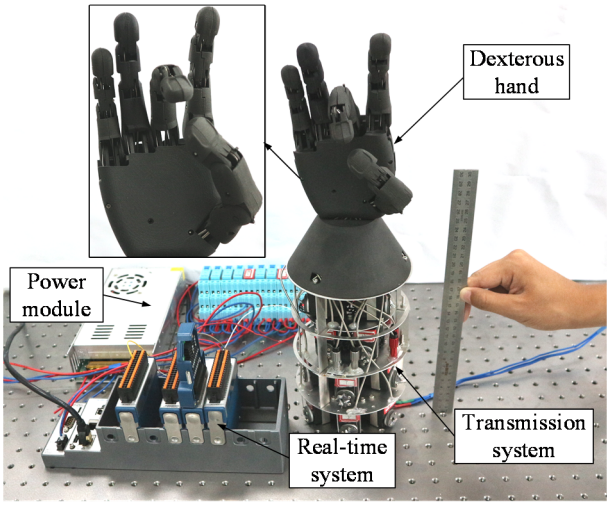

Fig. 2 19-Dofs Humanoid Hand

The index finger, middle finger, ring finger and little finger have the same degree of freedom and structure except the length of the joint. The finger is mainly composed of four joints. In addition to the base joint, a return torsion spring is installed at the other joints.

The base of the finger is hinged to the palm of the hand, and the entire finger transmits power through the five wire ropes and the pulley of each joint. The structure of the thumb is similar to the structure of the index finger, with only one middle finger joint missing and the rest being identical.

III. THE DESIGN UNDER THE MAXIMUM GRAB SPACE

The factors that can increase the performance of manual capture operations are usually the following: Is there a sufficient number of fingers. Whether the finger has a large operating space. Whether the palm has the ability to adjust the posture between the fingers according to the grasping task. Whether the thumb with the pair has enough interaction ability with the index finger, middle finger, nameless and little finger.

For the dexterous hand fingers, the motion space can be mathematically described by mathematical tools, and the mapping relationship between the fingertip Cartesian space and the joint space can be used as the theoretical basis of the control system and the grab operation.

A single finger can be regarded as a multi-joint series-level robot. Therefore, the joint coordinate system of the index finger is established according to the robot theory and the finger structure model.

The D-H method is used to establish the finger coordinate system $X_0Y_0Z_0$ as the fixed reference frame coordinate, and the rest is the moving coordinate. The length of each knuckle is a1, a2, a3, a4.

The linear mapping relationship between joint velocity and fingertip position is expressed by the Jacobian matrix, that is, the relationship between the differential motion of the mechanism and time, expressed by $J(\theta)$. The Jacobian matrix can be used to judge the singular configuration of dexterous hands as well as velocity decomposition and moment decomposition, which play an irreplaceable role in the control of dexterous hands.

A. *Knuckle length optimization*

The dexterity of the robot is an important indicator of the quality of the organization. The dexterity is good, the efficiency of the operation of the mechanism is high and the operation is stable, the working components can be well coordinated, and the predetermined motion relationship between the input and the output is ensured; On the other hand, if the dexterity of the mechanism is poor, the output will have a large distortion between the input and the input, and the components cannot guarantee a good coordination work. Over time, the motion life of the mechanism will be greatly reduced. Therefore, studying the dexterity performance of robots is an important consideration at the beginning of robot design.

The positional arrangement of the thumb determines the shape of the thumb and the gripping ability of the entire palm. There are two main angles affecting the position of the thumb in the design of the thumb structure: the angle θ between the thumb and the middle finger and the palm of the hand, and the torsion angle α of the proximal and middle finger joints of the thumb. In this paper, the Jacques condition number index is used as the dexterity performance evaluation index of the dexterous hand to optimize the torsion angle α.

B. *Jacques condition number evaluation index*

The relationship between the velocity vector $\dot{\boldsymbol{\Theta}}$ of the joints of the dexterous hand and the speed V of the tip point p is:

$$\boldsymbol{V} = \boldsymbol{J}\dot{\boldsymbol{\Theta}} \tag{1}$$

Where J is the Jacobian matrix.

Assume that the speed $\dot{\boldsymbol{\Theta}}$ of each joint changes $\Delta\dot{\boldsymbol{\Theta}}$; Then the fingertip velocity produces a deviation ΔV, which is expressed as:

$$\boldsymbol{V}+\Delta\boldsymbol{V}=\boldsymbol{J}\left(\dot{\boldsymbol{\Theta}}+\Delta\dot{\boldsymbol{\Theta}}\right) \tag{2}$$

Which is:

$$\Delta\boldsymbol{V}=\boldsymbol{J}\Delta\dot{\boldsymbol{\Theta}} \tag{3}$$

Calculate the norm for the above formula:

$$\begin{cases}\|\Delta\boldsymbol{V}\|=\|\boldsymbol{J}\Delta\dot{\boldsymbol{\Theta}}\|\le\|\boldsymbol{J}\|\|\Delta\dot{\boldsymbol{\Theta}}\| \\ \|\dot{\boldsymbol{\Theta}}\|=\|\boldsymbol{J}^{-1}\boldsymbol{V}\|\le\|\boldsymbol{J}^{-1}\|\|\boldsymbol{V}\|\end{cases} \tag{4}$$

Simultaneously, we know:

$$\frac{\|\Delta\boldsymbol{V}\|}{\|\boldsymbol{V}\|}\le\|\boldsymbol{J}\|\|\boldsymbol{J}^{-1}\|\frac{\|\Delta\dot{\boldsymbol{\Theta}}\|}{\|\dot{\boldsymbol{\Theta}}\|} \tag{5}$$

$\|\boldsymbol{J}\|\|\boldsymbol{J}^{-1}\|$—Jacques matrix condition number. Known by the norm definition: $1\le cond\,(\mathrm{J})\le\infty$.

The condition number of the Jacobian matrix reflects the ill-conditioned degree of the matrix. The larger the value of the Jacobian matrix condition, the higher the sensitivity to small changes. When calculating, the distortion occurs between the output and the input.

For the convenience of research, this paper uses the reciprocal of the condition number of the Jacobian matrix as the thumb evaluation index:

$$0\le\frac{1}{cond\left(\boldsymbol{J}\right)}=\frac{\sigma_m}{\sigma_n}\le 1 \tag{6}$$

Where σ_m is the Jacobian matrix maximum singular value, σ_n is the Jacobian matrix minimum singular value.

The condition number of the Jacobian matrix is not a fixed value, but varies according to the joint variables of the mechanism. Therefore, it is inaccurate to measure the performance index of a mechanism with a specific bit pattern. Based on the consideration of the workspace, Gosselin proposed the Global Conditioning Index:

$$G=\frac{\int_{\Omega}\frac{1}{cond\left(\boldsymbol{J}\right)}d\Omega}{\int_{\Omega}d\Omega} \tag{7}$$

Where G is the Global Conditioning Index, Ω is the Reachable workspace.

It can be known from Eq. (7) that the mathematical meaning is the numerical average of the condition number index in the reachable workspace of the mechanism. Therefore, in order to obtain global performance indicators, all the conditions in the organization's workspace must be calculated.

According to the conditional number of the Jacobian matrix, it is generally difficult to calculate the analytical solution, and the integration process up to the working space is complicated. Therefore, the discrete performance index is selected to approximate the global performance index:

$$G=\frac{\sum_{i=1}^{N}\frac{1}{cond\left(J\right)}}{N} \tag{8}$$

Where N is the number of samples up to the workspace.

IV. Flexibility and Crawling Experiments

A. Jacques condition number evaluation index calculation

The program is written in MATLAB to obtain the performance spectrum of the Jacobian matrix condition number dexterity index as a function of the length of the member.

Since the torsion angle α is only related to the proximal and middle finger joints, according to the length of the thumb of the human hand: the length of the middle phalanx is L_2=20 mm, and the length of the distal phalanx is L_3=20 mm. According to MATLAB, the relationship between the condition number index and the torsion angle α is solved

As the torsion angle α becomes larger, the value of the condition number index is larger, which is almost independent of the rod length L1. Since 0°≤α≤90°, when the twist angle α is equal to 90°, the condition number index is the largest, and the dexterity of the finger is the best.

For the anthropomorphic nature of the dexterous hand, according to the length of the middle phalanx and distal phalanx of the thumb, the proximal phalanx L_1=23 mm is taken.

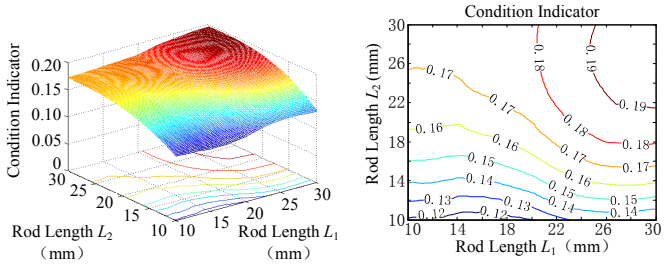

(a) L_3=20mm

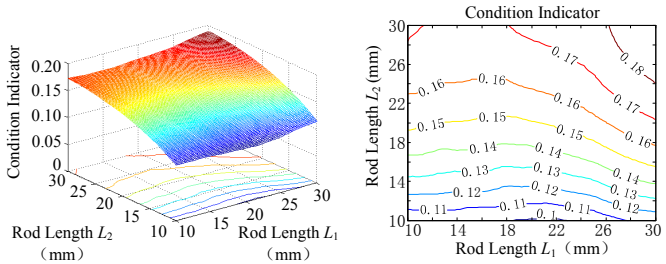

(b) L_3=25mm

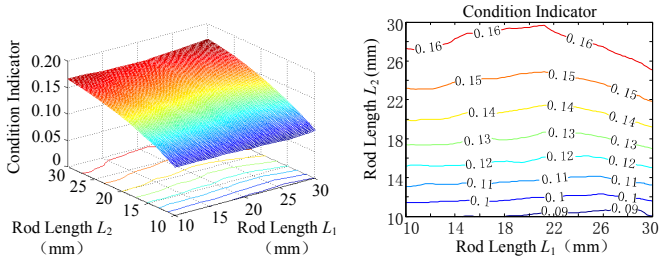

(c) L_3=30mm

Fig. 3 Different L3's Jacobian matrix condition number dexterity index

The medium-high line value in Fig. 6 represents the reciprocal of the condition number of the Jacobian matrix. Since the condition number of the Jacobian matrix is always greater than 1, the larger the reciprocal value, the closer the

current value is to 1, the better the dexterity of the dexterous hand.

In Fig.3, (a)-(c) respectively indicate the performance map of the condition number index of the Jacobian matrix as L_1 and L_2 change when the distal knuckle length L_3 is 20 mm, 25 mm, and 30 mm.

Observe the three sets of data in the figure to see: when L_3=20mm and L_1=L_2=25mm, the dexterity hand's Jacques matrix condition number index is the highest, indicating that the dexterity of the dexterous hand is the best at this point, and the speed isotropic is optimal, the same below;

When L_3=25mm and L_1=L_2=27mm, the dexterous hand has the highest index of the Jacques matrix condition.

When L_3=30mm, the length change of L_2 plays a decisive role in the performance index. When L_1=21.5mm and L_2=29.4mm, the dexterity hand has the highest Jacques matrix condition index.

Analysis of the three sets of data in Fig. 6 presents the following characteristics;

(a) When the joints are elongated, the value of the condition number of the Jacobian matrix is getting smaller and smaller, indicating that the dexterity is getting worse and worse, and the isotropic performance of the motion transmission is reduced;

(b) As the length of the joint increases, L2 plays a decisive role in the value of the condition number index of the Jacobian matrix;

(c) When the lengths of the drive rods tend to be the same, the isotropic transmission is better, and the minimum speed transmission is larger.

B. Angle of thumb and palm

In the process of grasping the dexterous hand, it is divided into two modes: precise capture and strong capture. Envelope capture is mainly used in strong crawling. According to the characteristics of the human hand, it is inevitably closed in the process of capturing the largest object. In daily life, the enveloping objects of the human hand are mainly large cylinders and spheres. This article takes the example of grabbing a cylinder as an example[13]..

The thumb of the hand is extremely flexible and complicated. In order to increase the similarity with the human hand and ensure the ability to grasp the object at the maximum, it is necessary to optimize the angle θ between the thumb and the palm, and the length of the three joints of the middle finger. In this section, the dexterous hand is used to grasp the cylinder to optimize the middle finger knuckle and θ. The non-complete closure during the grasping process means that the distance between the fingertip of the middle finger and the fingertip of the thumb in the X and Y directions is ΔX, ΔY, as shown in Fig. 4.

The larger the value of θ, the worse the anthropomorphism, but the larger the radius R of the maximum gripping cylinder. On the contrary, the smaller the value of θ, the better the anthropomorphism, and the smaller the maximum radius R of the grasping cylinder. It can be seen that θ and R cannot simultaneously reach the optimal solution.

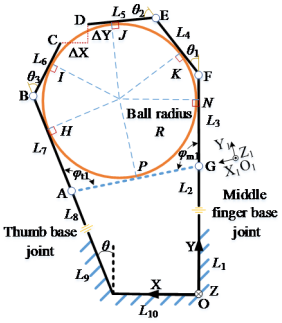

Fig. 4 Thumb and middle finger envelope capture

In a given reference coordinate system, a set of point contact definitions can be used to grab G={p_1,p_2, ⋯ ,p_m}, Where p_1, p_2,…, p_m are contact point vectors, represented by the unit normal vector n and the vector diameter r_0 at the contact point of the finger, which is：

$$\boldsymbol{p}=\begin{bmatrix}\boldsymbol{n}\\ \boldsymbol{r}_0\times\boldsymbol{n}\end{bmatrix} \tag{9}$$

The shape-closed discriminant function $J_0(G)$ defining the multi-finger grab is the minimum of the following linear programming problem.

$$J_0(\boldsymbol{G})=\min_{\Omega_0}\sum_{j=1}^{n+1}y_j \tag{10}$$

Where the feasible set Ω_0 is represented by the following constraints：

$$\begin{cases}\sum_{i=1}^{m}\lambda_i\boldsymbol{p}+\boldsymbol{y}=0\\ \sum_{i=1}^{m}\lambda_i+y_{n+1}=1\\ \lambda_i,y_j\ge 0,i=1,2,\ldots,m;j=1,2,\ldots,n,n+1\end{cases} \tag{11}$$

Where y is the $[y_1, y_2, \ldots y_n]^T$, y_{n+1} is the manual control variable, λ is the solution vector, m is the number of contact point line vectors p, n is the dimension of the contact point line vector p.

The point O is taken as the reference coordinate system origin, and $X_0Y_0Z_0$ is taken as the reference coordinate system, and the thumb, the middle finger and the cylinder are tangent to the points H, I, J, K, N and P. According to the analysis, the function $G_\theta(M)$ of θ with respect to L_3, L_4, L_5, θ_1, θ_2 and θ_3 is obtained:

$$G_\theta(\boldsymbol{M})=\{\theta(L_3,L_4,L_5,\theta_1,\theta_2,\theta_3)\} \tag{12}$$

$$s.t\begin{cases}\left(L_{10}+\varpi\cos\theta+L_6\cos(\theta+\theta_3)\right)-\mu\le\varepsilon\\ \left(L_1+L_2+L_3+\upsilon\right)-\left(\varpi\sin\theta+L_6\sin(\theta+\theta_3)\right)\le\varepsilon\\ L_9+L_8+L_7=\varpi\\ L_4\cos\theta_1+L_5\cos(\theta_1+\theta_2)=\upsilon\\ L_4\sin\theta_1+L_5\sin(\theta_1+\theta_2)=\mu\end{cases}$$

Where ε is the distance limit, ϖ is the length of the thumb phalanx on the same axis, θ is the angle between the base of the thumb and the plane of the palm, υ is the length of the L_4 and L_5 on the Y axis, μ is the length of the L_4 and L_5 on the X axis, R is the envelope grabs the radius of the cylinder, $Li(i=1,2,\ldots,10)$ is the structural length of the dexterous hand thumb, middle finger and palm;

$$H_R(\boldsymbol{M})=\{R(L_3, L_4, L_5, \theta_1, \theta_2, \theta_3)\} \tag{13}$$
$$s.t\begin{cases} R\left(\tan\left(\theta_1/2\right)+\tan\left(\theta_2/2\right)\right)=L_4 \\ R\left(\tan\left(\theta_3/2\right)-\tan\left(\theta_2/2\right)\right)=L_6-L_5 \end{cases}$$

In summary, the objective function of the dexterous hand grabbing cylinder is:

$$F(\boldsymbol{M})=\min\left\{\min\left\{G_\theta(\boldsymbol{M})\right\}+\max\left\{H_R(\boldsymbol{M})\right\}+\sum_{i=1}^{n+1}y_j(\boldsymbol{M})\right\}$$
$$s.t\begin{cases} \sum_{i=1}^{m}\lambda_i\boldsymbol{p}+\boldsymbol{y}=0 \\ \sum_{i=1}^{m}\lambda_i+y_{n+1}=1 \\ \lambda_i, y_j\geq 0, i=1,2,\ldots,m; j=1,2,3 \\ \boldsymbol{M}=\left[L_3、\ L_4、\ L_5、\ \theta_1、\ \theta_2、\ \theta_3\right]^{\mathrm{T}} \end{cases} \tag{14}$$

On the multi-objective optimization problem, there are often several problems in which nonlinear targets are simultaneously optimized, and the targets conflict with each other. Therefore, the solution of the equation is not the optimal solution of all the targets, but the optimal solution of the target based on a certain weight. In the constraint function, there is a nonlinear equation. In the solution process of the optimal solution, multi-objective optimization problem solving is needed.

The differential evolution algorithm is used to iterate, the population number is 100, the mutation rate is 0.85, the crossover rate is 0.9, the differential evolution method option is standard variation, the local search step size is 100, and the convergence condition is twice before and after the iteration difference is less than 10^{-5}.

The convergence trend of the objective function is shown in Fig. 5. It can be seen from the figure that the objective function converges faster with the optimization process of the algorithm. According to the length of the knuckles of each finger, the target optimization can be obtained: θ=0.7854rad, R=35.5823mm.

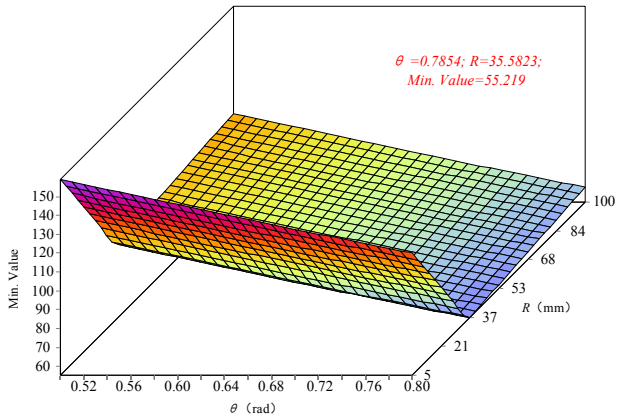

Fig.5 Objective function graph

V. FLEXIBILITY AND CRAWLING EXPERIMENTS

The convergence trend of the objective function is shown in Fig. 5. It can be seen from the figure that the objective function converges faster with the optimization process of the algorithm. According to the length of the knuckles of each finger, the target optimization can be obtained: θ=0.7854rad, R=35.5823mm.

A. Flexibility experiment

The reason why the human hand can complete all kinds of grasping tasks is entirely due to the flexible movement of the fingers and the large bending deformation ability of the fingers. Under the action of the hand muscles and tendons, the maximum bending angle of each finger to the palm can reach 180°, so that the envelope of the target grab can be formed. Therefore, the bending amplitude of the finger determines the operational performance of the hand to a certain extent. As shown in Fig. 6, the swing degree of freedom has a swing amplitude of ±15°, and the swing of the thumb can reach plus or minus 90°. Each curved joint can be bent 90°, and each finger can be bent by 180°.

Being able to make various gestures is an important indicator of the flexibility of the dexterous hand. This article selects the common gestures in life to verify the dexterous hand. It is a commonly used digital gesture in northern China, and each gesture fully utilizes five fingers. For example, the number ten makes full use of the bending ability of each finger, and the number five utilizes the degree of freedom of finger swing. As shown in Fig. 6, the dexterous hand is very good at making various gestures. In addition to the digital gestures, the orchid finger and the rock gesture can also be easily made, indicating that the dexterous hand of the design has great flexibility.

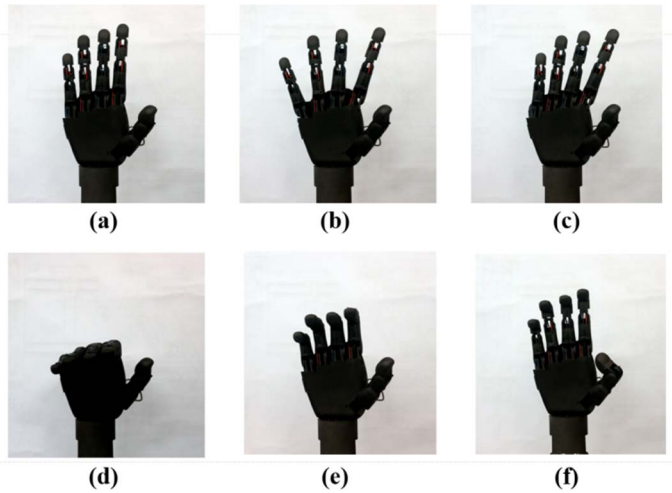

Figure 6 Dexterity hand degree display

B. Grab experiment

Grab ability is one of the important abilities of dexterous hands. Common objects include columnar bodies, spheres, and tiny objects. As shown in Fig.7, the grasping ability of dexterous hands is verified. Experiments have captured mineral water bottles, apples and peanuts. The verification results show that the dexterous hand has a good grasping ability and can effectively capture various objects.

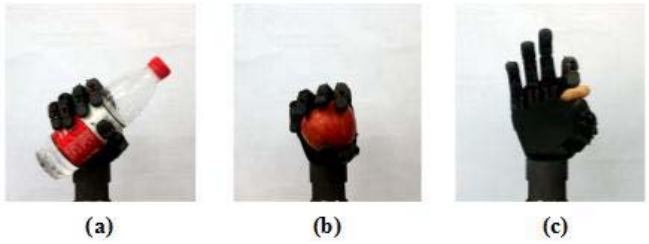

Figure 7 Physical capture

IV. Conclusion

As the end operator of the robot, dexterous hand is a very important part of the robot system. Its performance directly determines the robot's controllability and intelligence level. This paper designs a new five-finger bionic dexterous hand with a total of 19 degrees of freedom, in which the thumb has 3 degrees of freedom, and the remaining fingers are 4 degrees of freedom. A kinematic model was established, and the joint torsion angle and joint length were optimized using the Jacques condition number index. The differential evolution algorithm was used to optimize the angle between the thumb and the palm. Experiment test varied posture under no-load conditions, and verify the flexibility of the dexterous hand. After testing its gripping ability, it has verified the dexterous hand has large gripping range and good adaptability when grabbing spheres, sheets and cylinders of different sizes.

The current work lays the foundation for further research and development of dexterous hands, there are many areas that are imperfect and require further research: 1) This paper uses a new transmission method based on the traditional tendon transmission. The principle and reliability of this transmission method need to be further verified; 2) The load capacity of the grab is an important indicator for dexterous hand, and can be improved by optimizing the stiffness of the structure; 3) It is necessary to achieve dexterous hand high-precision position control by installing a potentiometer on the finger joint and optimizing the control strategy; 4) A flexible force sensor can be added on the surface of hand to achieve force compliance control; 5) The more freedom of the system, the higher the risk of failure. Considering the completion of common tasks can reduce the complexity of the hand and reduce the degree of freedom. 6) The application of the hand needs to be coordinated with the arm, which is one of works in next step.

REFERENCES

[1] Dogar M R , Srinivasa S . *Push-Grasping with Dexterous Hands: Mechanics and a Method* [C]. IEEE/RSJ International Conference on Intelligent Robots & Systems. IEEE, 2010.

[2] Nixon Dutta, Joyeta Saha, Faysal Sarker, et al. A Novel Design of a Multi- DOF Mobile Robotic Helping Hand for Paralyzed Patients[C]. *Proceedings of the 7th International Conference on Computing, Communications and Informatics (ICACCI)*, Bangalore, INDIA, SEP, 2018:19-22.

[3] Chen, Zhaopeng , et al. "Cartesian Impedance Control on Five-Finger Dexterous Robot Hand DLR-HIT II with Flexible Joint[C]."Intelligent Robotics and Applications - Third International Conference, ICIRA 2010, Shanghai, China, November 10-12, 2010. Proceedings, Part I.DBLP, 2010.

[4] TAO Guoliang, XIE Jianwei, ZHOU Hong. Research achievements and development trends of pneumatic artificial muscles [J]. Journal of Mechanical Engineering, 2009, 45(10):75-83.

[5] Townsend, William. "The BarrettHand grasper programmably flexible part handling and assembly [M]."Industrial Robot An International Journal, 2000, 27(3):181-188.

[6] Kawasaki H, Komatsu T, Uchiyama K, et al. Dexterous anthropomorphic robot hand with distributed tactile sensor: Gifu hand II [C]. IEEE International Conference on Systems. 1999.

[7] Anderson, Robert J. "Advanced dexterous manipulation for IED defeat : report on the feasibility of using the ShadowHand for remote operations. " Office of Scientific & Technical Information Technical Reports (2011).

[8] Takayama, Toshio , Y. Chiba , and T. Omata . "Tokyo-TECH 100 N Hand : Three-fingered eight-DOF hand with a force-magnification mechanism." 2009 IEEE International Conference on Robotics and Automation, ICRA 2009, Kobe, Japan, May 12-17, 2009 IEEE, 2009.

[9] Schulz S, C Pylatiuk , and G. Bretthauer . "A New Ultralight Anthropomorphic Hand." IEEE International Conference on Robotics & Automation IEEE, 2003.

[10] Baker, William , et al. "Robonaut 2 and you: Specifying and executing complex operations." Advanced Robotics & Its Social Impacts IEEE, 2017.

[11] Lotti F, P Tiezzi , and G. Vassura . "UBH3: investigating alternative design concepts for robotic hands." Automation Congress IEEE, 2004.

[12] Chaigneau D, Arsicault M, Gazeau J P, et al. LMS robotic hand grasp and manipulation planning (an isomorphic exoskeleton approach). Robotica, 2008, 26(2):177-188.

[13] Hu MW, Wang HG, Pan XA, et al. Research on elastic deformation modeling of collaborative robots[C]//2017 ROBIO. Macau, China: IEEE, 2017: 2462-2467.